Article:
Hine, PJ and Gusev, AA (2019) Validating a micromechanical modelling scheme for predicting the five independent viscoelastic constants of unidirectional carbon fibre composites. International Journal of Engineering Science, 144. UNSP 103133. ISSN 0020-7225

https://doi.org/10.1016/j.ijengsci.2019.103133

Validating a micromechanical modelling scheme for predicting the five independent viscoelastic constants of unidirectional carbon fibre composites

P.J.Hine[1] and A.A.Gusev[2]

1- Soft Matter Group, School of Physics and Astronomy, University of Leeds, Leeds, LS2 9JT, UK

2 - Institute of Polymers, Department of Materials, ETH Zürich, 8093 Zürich, Switzerland

Abstract

In this paper we experimentally validate a new micromechanical modelling scheme for predicting the five independent viscoelastic constants of a unidirectional carbon fibre epoxy resin composite. This study has built on a number of previous papers by these authors, where extensive finite element calculations were used to validate a much more easily implemented, classical analytical micromechanical approach for predicting the viscoelastic properties of composite materials. For formulating the viscoelastic predictions, the elastic-viscoelastic correspondence principle is used to convert the static elastic solutions to their complex steady state viscoelastic forms simply by replacing static elastic moduli of the matrix and the fibers by their complex viscoelastic moduli

To formulate accurate micromechanical predictions for comparison and validation by experimental measurements, appropriate values for the five independent elastic constants of the reinforcing carbon fibres in the experimental materials are required. To obtain them, we have used the ultrasonic immersion method (UIM) and an inverse modelling scheme as previously described by Smith. The UIM allows the full stiffness tensor to be determined for both the carbon fibre composite and the epoxy resin matrix at a frequency of 2.25MHz. The validated Hashin-Rosen composite cylinders micromechanical model was then used to

determine the best fit elastic constants of the carbon fibres. Once these were determined, the 'viscoelastic properties' of both the pure epoxy matrix and the carbon fibre composite were studied using low frequency measurements (1Hz). The results showed that for the two viscoelastic constants that can be routinely measured experimentally, namely the longitudinal and transverse Young's moduli, these are very well predicted by the same micromechanical model. Most importantly, following this validation, the micromechanical model can then easily provide all of the five independent viscoelastic composite stiffness constants. These values are critical for accurate vibration damping and noise cutting design of advanced engineering composite parts exposed to oscillatory loading such as aircraft wings and tails or wind turbine blades.

1 Introduction

Carbon fibre composites are being increasingly used in a wide range of applications that make use of the excellent specific stiffness and strength properties of these materials. Amongst these include commercial and military aircrafts [1], high performance automotives [2, 3] and wind turbine blades [4, 5]. A common theme to these applications is that they are routinely subjected to oscillating or vibrational loading [6], meaning that the damping properties of these composite materials can be equally as important as their elastic stiffness constants (which is fairly often taken as the exclusive driver for composite design). In fact, it can be stated that if the viscoelastic properties of these composite materials were more readily understood, or more pertinently if they could be accurately predicted, then more optimal, viscoelastic design solutions could be attained in these increasingly important end uses. For this, analytical theoretical solutions available for laminated composite plates and shells [7-9] and then converted to the viscoelastic domain using the elastic-viscoelastic correspondence principle

[10] could be employed to achieve more optimal, viscoelastic design solutions. Alternatively, numerical finite element calculations (e.g., by calculating the natural frequencies and the corresponding mode shapes of damped structural vibrations directly in the frequency domain using complex arithmetic solvers [11-14]) could be used in the same way.

As far as we are aware, there is very little published on the prediction (and experimental validation) of the viscoelastic properties of unidirectional composites. In particular on a method to obtain all five independent viscoelastic constants (both the real and the imaginary components, which are often termed as the storage and the loss moduli, respectively) which are required for designers. One of the critical reasons is that the loss moduli of carbon fibre composites are two to four orders of magnitude smaller than their respective storage moduli so it is experimentally demanding to measure the loss moduli accurately. Nonetheless, despite their relatively small values, it is exactly these loss moduli that determine the vibration damping and noise cutting performance of advanced engineering structures from such composite materials (airplane wings and tails, wind turbine blades, racing cars spoilers, etc.).

The research presented here was split into two distinct segments, both of which used a combination of micromechanical modelling and experimental measurements. In the first procedure, following the strategy proposed by Smith [15], the ultrasonic immersion technique was used to determine the elastic properties of a unidirectional carbon fibres composite and its associated pure epoxy matrix component at a frequency of 2.25MHz. A previously validated [11], classical Hashin-Rosen's composite cylinders micromechanical model was then used to find the best 'fit' five carbon fibre constants to match the experimentally measured composite elastic constants. In the second part, the objective was to predict the viscoelastic constants of the same carbon fibre epoxy composite but at a much lower frequency of 1Hz, based on viscoelastic measurements of the epoxy matrix and the previously determined carbon fibre elastic constants. For validation purposes, experimental viscoelastic measurements were

carried out for two of the five viscoelastic constants of the composite, namely the in-plane longitudinal and transverse Young's moduli. Agreement between the micromechanical predictions and the experimental measurements for these two viscoelastic engineering moduli (for both their storage and loss parts) was excellent within the experimental uncertainties, validating the approach and also offering predictions of all five viscoelastic constants, some of which are very difficult to measure experimentally.

2 Experimental

2.1 Materials

The unidirectional composite used in this study comprised Hexcel AS4 carbon fibres [16] in a 913 epoxy resin [17]. Importantly, in addition to a cured composite sample (made using the recommended manufacturer's conditions) a sample of the pure epoxy resin (made using the same processing conditions) was also obtained. Typical values given by the manufacturers for these two materials are shown in Table 1. It should be noted that Young's moduli will be measured independently in this work at the two relevant measurement frequencies: a high ultrasonic frequency of 2.25Mhz for determining the carbon fibre **elastic** constants and a lower frequency of 1Hz for predicting and validating the composite **viscoelastic** constants. It is worth a comment at this point regarding these two different test frequencies used. For determining the carbon fibre elastic constants, the ultrasonic immersion test was chosen (2.25MHz), as it allows for the determination of all five independent elastic constants of the carbon fibres (and the carbon fibre constants are not significantly frequency dependent). However, for evaluation the elastic constants of a typical carbon fibre reinforced epoxy laminate, a more representative frequency of 1 Hz was used, as the epoxy resin matrix elastic constants are significantly frequency dependent.

	AS4 carbon fibre	913 epoxy resin
Young' Modulus (GPa)	231	3.39
Density (kg/m^3)	1800	1230

Table 1: Typical manufacturer's values for AS4 carbon fibre and 913 epoxy resin for reference (test frequency and method unknown).

Accurate density measurements on a large sample cut from the composite plate, together with the density values for the two component phases shown in Table 1 above, gave a measured value for the fibre volume fraction of 0.58 using the density rule of mixtures. This value was also verified using the image analysis procedure to measure the fraction of the fibres, see Figure 1.

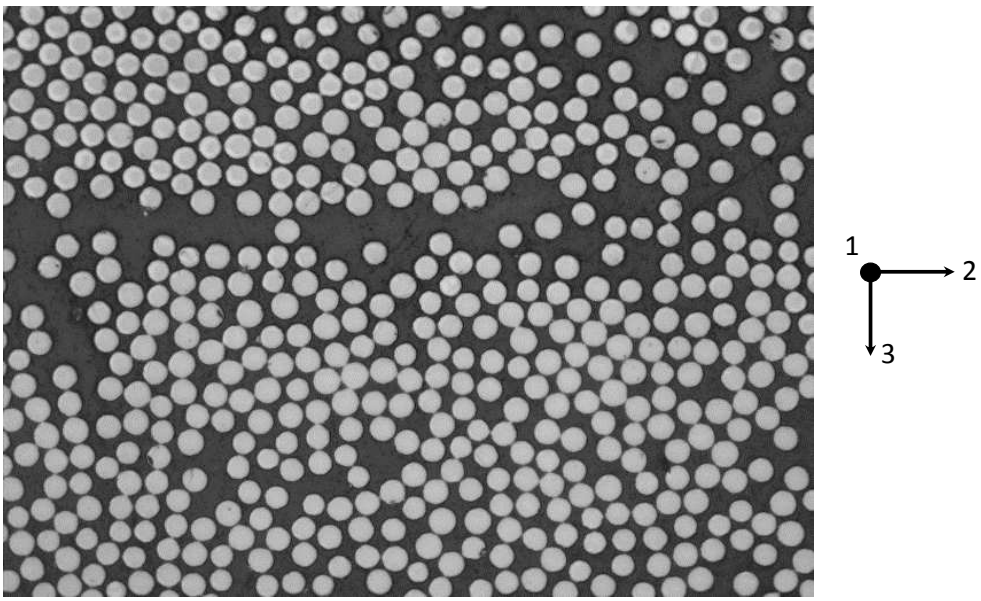

Figure 1: Typical cross section through the unidirectional carbon fibre epoxy composite (bottom length = 200μm).

2.2 Experimental testing methods

2.2.1 Ultrasonic immersion method

In a number of previous studies, aimed at developing and validating both analytical, numerical and finite element models to understand the elastic properties of fibre reinforced composites, this group has made extensive use of the ultrasonic immersion method (UIM) [15, 18]. This is due to the ability of the technique to measure simultaneously the five individual elastic constants of a unidirectional fibre composite material (as the off axis terms of the stiffness matrix can often be difficult to measure by traditional static techniques). The first use of the technique at Leeds was described in detail in the work of Dyer [19] and the PhD study of Lord [20], which were based upon the seminal works of Markham [21], Smith [15] and Read and Dean [18]. Such studies included understanding negative Poisson's ratios in angle ply laminates [22, 23], extracting the elastic constants of anisotropic polymeric fibres [24, 25] and investigating the effects of random transverse packing in unidirectional fibre composites [26].

In the UIM, the sample to be studied is placed between ultrasonic transducers (2.25MHz) in a temperature controlled water both (set at 30.0 ± 0.1°C). By measuring the difference in the arrival time with and without a sample in the transducers path, the velocity of the sound wave in the sample can be determined. The unique aspect of the technique is that if the sample is rotated at a critical angle, then the longitudinal sound wave from the transmitter is converted into a shear wave in the sample (termed mode conversion). In this way the velocity of both the longitudinal wave (V_L) and the shear wave (V_S) can be investigated.

The previously published papers showed that these two wave velocities are controlled by the four elastic constants in the plane of the propagation of the two waves and the direction of travel in the plane (given by the angle of refraction r).

For example, for propagation in the 23 plane (see Figure 2), the following two relationships predict the variation in sound wave speed with elastic constants and the angle of wave propagation in the sample (angle of refraction r).

$$V_L{}^2 = \frac{B_{22} + B_{33} + \left[(B_{22} - B_{33})^2 + 4B_{23}{}^2\right]^{\frac{1}{2}}}{2\rho} \quad (1)$$

$$V_S{}^2 = \frac{B_{22} + B_{33} - \left[(B_{22} - B_{33})^2 + 4B_{23}{}^2\right]^{\frac{1}{2}}}{2\rho} \quad (2)$$

where $B_{22} = C_{22}cos^2 r + C_{44}sin^2 r$

$B_{33} = C_{33}sin^2 r + C_{44}cos^2 r$

$B_{23} = (C_{44} + C_{33})sin\, r\, cos\, r$

r is the angle of sound propagation in the composite sample and ρ is the sample density.

Once the dependence of the two sound velocities (V_L and V_S) is determined with respect to r, a computer programme finds the 'best' values of the four stiffness constants to fit the data. To obtain a full set of composite elastic constants (and hence determine the elastic constants of the carbon fibres), three experiments for sound propagation in the 23, 13 and 12 planes are required, as shown schematically in Figure 2. Here the 1 axis is the fibre direction. For propagation in the 12 plane, strips were cut from the composite panel and then glued together with the 1 axis to the front to create a sample of sufficient dimensions to carry out the experiment in the 12 plane.

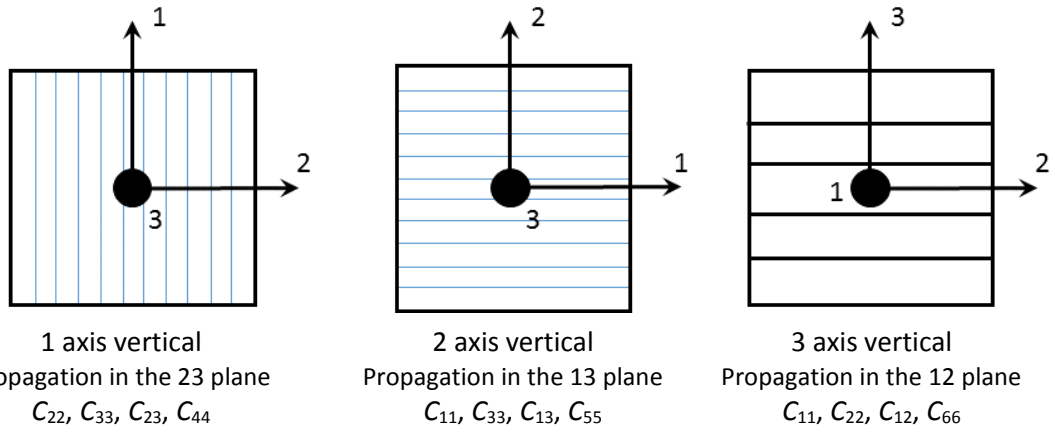

Figure 2: The three planes of propagation for the UIM experiments and the stiffness constants derived for each. For the left and middle diagrams, the blue lines indicate the fibre direction. For the diagram on the right, the lines indicate that the sample is composed of several sample strips cut and reassembled.

The ultrasonic immersion method was also used to determine the elastic constants of a sample of the pure 913 epoxy resin at the same frequency (2.25MHz). As this sample was isotropic, this required only one plane of propagation.

2.2.2 Dynamical mechanical testing

Pure epoxy resin sample

For informing the viscoelastic micromechanical predictions at a lower frequency (1Hz), dynamic mechanical analysis experiments were carried out (DMA). In order to carry out the micromechanical predictions, two independent viscoelastic constants were required. The viscoelastic torsion properties (shear modulus G and tanδ) were determined using a rectangular geometry and a Rheometrics RDSII. The viscoelastic tensile properties (Young's modulus E and tanδ) were determined in three-point bend also using a Rheometrics RDAII. Both tests were carried out at room temperature (20°C) and a frequency of 1Hz.

Composite samples

DMA viscoelastic measurements were also carried out on the unidirectional composite samples in both the longitudinal direction (1 axis) and the transverse direction (2 axis) using a three-point bend geometry (span = 48mm) at the same frequency of 1Hz.

3 Micromechanical modelling

3.1 Inverse calculation for determining the carbon fibre elastic constants

3.1.1 Transversely isotropic material

The stiffness of a transversely isotropic material is completely described by a set of five independent elastic moduli, e.g., C_{11}, C_{12}, C_{22}, C_{23}, and C_{55}. However, in many practical situations, this is not necessarily the most convenient form of stiffness characterization. For this reason, directly measurable engineering moduli are commonly used. In this work, the longitudinal Young's modulus (uniaxial modulus), Poisson's ratio under longitudinal load (major Poisson's ratio), longitudinal shear modulus, plane-strain bulk modulus, and transverse shear modulus are employed. In terms of the elastic moduli, they are expressed as, respectively

$$E_{11} = C_{11} - \frac{2C_{12}^2}{C_{22}+C_{23}} \quad \nu_{12} = \frac{C_{12}}{C_{22}+C_{23}} \quad G_{12} = C_{55} \quad k_{23} = \frac{1}{2}(C_{22} + C_{23}) \quad G_{23} = \frac{1}{2}(C_{22} - C_{23}) \qquad (3)$$

To simplify analytical results, υ_1 and υ_2 are used to designate matrix and fiber volume fractions, respectively, and shorthand notations

$$E = E_{11} \quad \nu = \nu_{12} \quad G = G_{12} \quad k = k_{23} \quad \mu = G_{23} \qquad (4)$$

are used for the engineering moduli of the two homogeneous phases, which are differentiated by using subscripts 1 and 2 for matrix and fibers, respectively.

3.1.2 Composite cylinders model

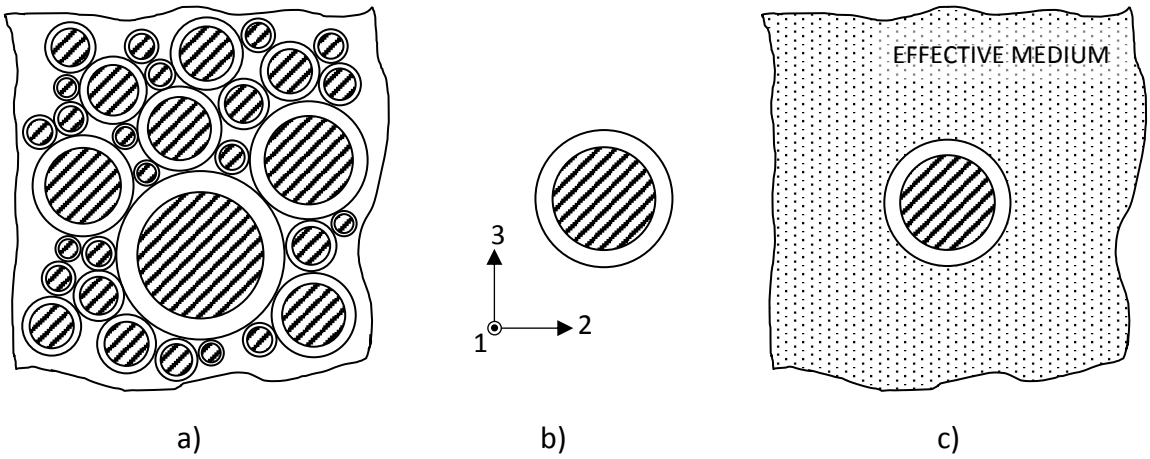

Figure 3: Composite cylinders model.

The composite cylinders model consists of a volume filling assemblage of infinitely long parallel composite cylinders of different radii down to infinitesimal, see Figure 3a. Each composite cylinder is made up of an inner circular fiber of radius a embedded in outer concentric matrix shell of radius b, see Figure 3b. The ratio of the two radii is chosen from $v_2 = (a/b)^3$ in order to reproduce the fiber volume fraction of the considered unidirectional composite. Then it follows that all such different composite cylinders have the same elastic moduli. For some certain uniform displacement boundary conditions such as axial extension, longitudinal shearing and radial displacement in the transverse plane, every composite cylinder behaves indistinguishably from some effective transversely isotropic homogeneous cylinder. For these boundary conditions, the related effective moduli are determined using known homogeneous elasticity solutions with the undetermined coefficients obtained from satisfaction of internal interface displacement and stress continuity conditions and external homogeneous boundary conditions, by requiring the average strain energy density in the composite cylinder be the same as in the equivalent homogeneous cylinder. The resulting effective moduli are given by

$$E_{11} = E_1 v_1 + E_2 v_2 + \frac{4(\nu_2 - \nu_1)^2 v_1 v_2}{v_1/k_2 + v_2/k_1 + 1/G_1} \tag{5}$$

$$\nu_{12} = \nu_1 v_1 + \nu_2 v_2 + \frac{(\nu_2 - \nu_1)(1/k_1 - 1/k_2) v_1 v_2}{v_1/k_2 + v_2/k_1 + 1/G_1} \tag{6}$$

$$G_{12} = G_1 + \frac{v_2}{1/(G_2 - G_1) + v_1/2G_1} \tag{7}$$

$$k_{23} = k_1 + \frac{v_2}{1/(k_2 - k_1) + v_1/(k_1 + G_1)} \tag{8}$$

where on the right hand side subscript 1 is matrix and 2 fibers. Exactly the same results are obtained using uniform traction boundary conditions so with regard to those four effective moduli, to an external observer the composite cylinder is indistinguishable from a homogeneous cylinder with the so-defined effective moduli.

However, for the transverse shear modulus the results obtained using the displacement and traction boundary conditions differ and a different approximation has been suggested by Christensen and Lo. In this Generalized Self Consistent Scheme (GSCS), see Figure 3c, a single composite cylinder is embedded in effective transversely isotropic material and homogeneous strain or stress boundary conditions are imposed at infinity. Satisfaction of interface continuity and boundary conditions at infinity yields sets of algebraic equations for determination of all five effective moduli. The results for E_{11}, ν_{12}, G_{12}, and k_{23} are precisely Eqs. (5) – (8). The remaining transverse shear modulus G_{23} is given implicitly, by the positive root of a quadratic equation with algebraically lengthy coefficients that are, however, easily suitable for numerical evaluation. It is shown that for all five moduli, the GSCS results are the same when using either stress or strain form homogeneous boundary conditions at infinity so to an external observer, for any arbitrary uniform deformation at infinity the composite cylinder behaves as a homogeneous cylinder with the transversely isotropic GSCS moduli.

Results (5) – (8) were first given by Hashin and Rosen [27], with Eqs. (5) and (6) presented in much more complicated but equivalent forms. Refined results (5) and (6) were given by

Hashin [28, 29]. The correct GSCS result for G_{23} was established later by Christensen and Lo [30].

3.2 Determination of the viscoelastic constants of the unidirectional composite

The elastic-viscoelastic correspondence principle is used to convert the above static elastic solutions to their complex steady state viscoelastic forms simply by replacing static elastic moduli of the matrix and the fibers by their complex viscoelastic moduli defined at a given oscillation frequency. It has recently been shown by Gusev and Kern [11] using a frequency domain finite element method, that direct numerical estimates of complex effective viscoelastic moduli of common carbon and glass fibre reinforced unidirectional composites are in excellent agreement with such classical analytical results. This recent work is a part of a broad research program [11-14, 31-34] that has demonstrated that the GSCS predictions are generally remarkably accurate and technologically very helpful for design of both elastic, viscoelastic and thermoelastic properties of fiber and particulate composites with both uncoated and coated inclusions.

4 Results

4.1 Determination of the **elastic** constants for the Hexcel AS4 carbon fibres using the ultrasonic immersion technique

In order to implement the inverse modelling scheme for determining the carbon fibre elastic constants, ultrasonic immersion measurements were carried out on the pure 913 epoxy sample and the composite plate. Figure 4 shows the measured longitudinal and transverse wave velocities versus the angle of wave propagation in the sample (r) for the pure epoxy sample. As expected, the velocities were found to be independent of the wave propagation angle,

confirming that the sample was isotropic. The dashed lines show the best simultaneous fit to Eqs. (1) and (2) (but for sound propagation in the 12 plane), which gave the following two independent elastic constants, C_{11} = 10.1GPa and C_{12} = 6.25GPa. This was a forced isotropic fit for the two elastic constants, using $C_{66} = (C_{11} - C_{12})/2$.

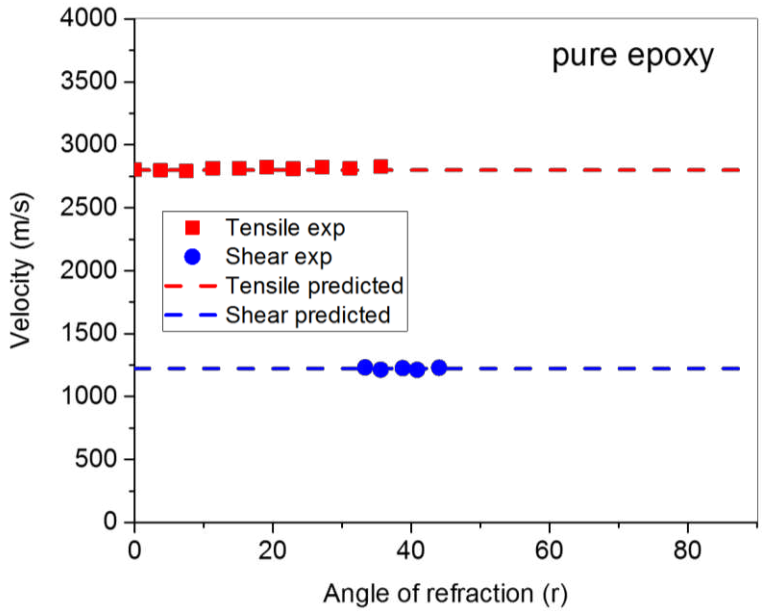

Figure 4: Longitudinal velocity (■) and transverse velocity (●) vs angle of refraction (r) for a pure epoxy 913 sample.

Next, the UIM experiments were carried out on the composite plate for wave propagation in the three planes shown in Figure 2, the results are shown in Figures 5 and 6. As for the pure epoxy, Eqs. (1) and (2) were simultaneously fitted to the measured velocity versus angle data. To aid fitting the results for the 13 plane, a value for the 90° point was added to the data set from the 0° measurement of the 12 plane. The isotropic plane (23 plane) was again fitted using a forced isotropic fit.

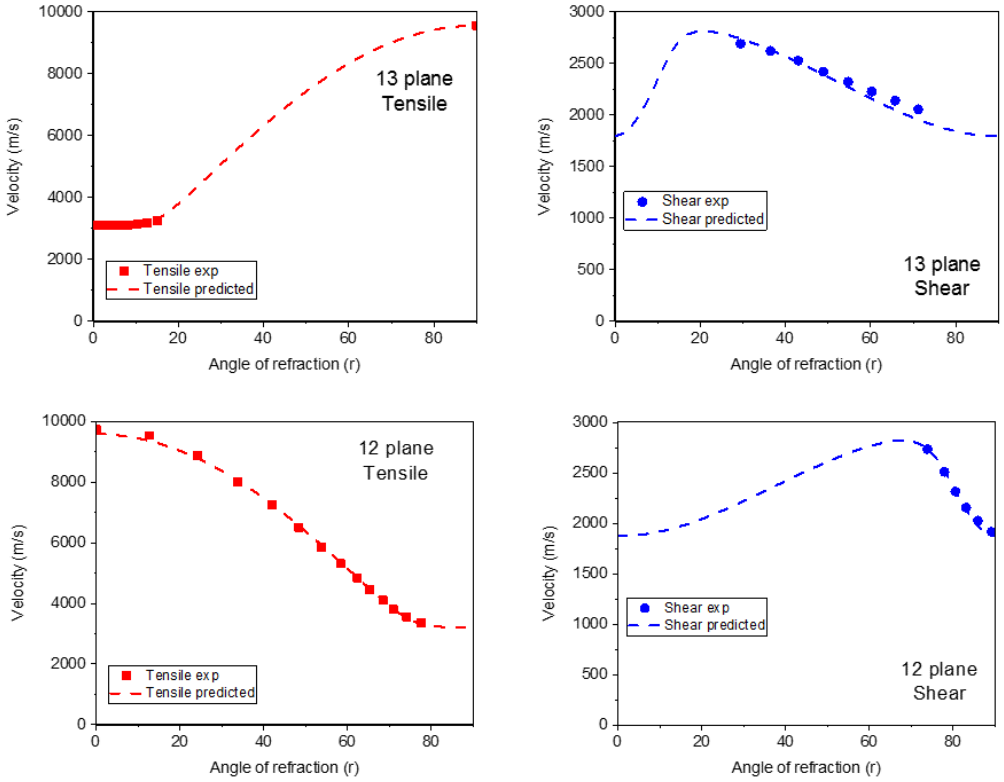

Figure 5: Longitudinal and transverse velocity vs angle of refraction for the unidirectional composite sample: top 13 plane, bottom 12 plane (1 is the fibre direction).

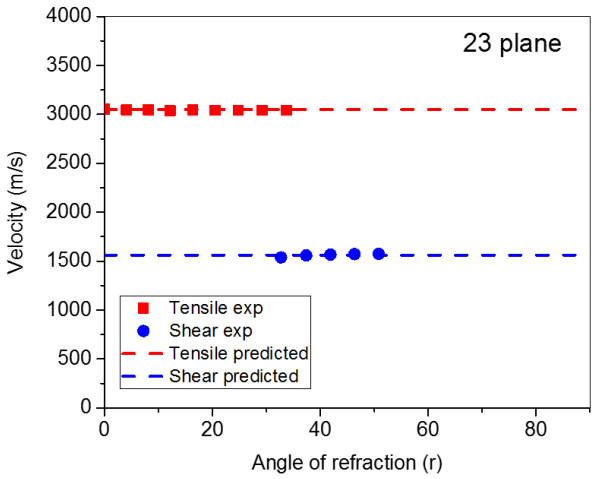

Figure 6: Longitudinal and transverse velocity vs angle of refraction for the composite sample: 23 plane.

Table 2 shows the fitted results for the five elastic constants of the unidirectional fibre reinforced epoxy composite (1 is the fibre direction) obtained by combining the measurements for the three propagation planes. A Voigt notation is used for the tensor components.

	C_{11}	C_{12}	C_{22}	C_{23}	C_{55}
(GPa)	138	7.40	14.2	6.70	5.1

Table 2: The best fit elastic constants for the unidirectional carbon fibre composite (Vf = 0.58) based on the ultrasonic measurements in the 13, 12 and 23 planes.

After carrying out the inverse modelling scheme using the Hashin and Rosen's composite cylinders model (as described in section 2), the five elastic stiffness constants for the individual carbon fibres were obtained as shown in Table 3. For convenience, Table 4 shows the derived engineering constants for the AS4 carbon fibres, which will be used in following viscoelastic studies.

	C_{11}	C_{12}	C_{22}	C_{23}	C_{55}
(GPa)	231	8.62	19.7	6.04	15.5

Table 3: The predicted AS4 carbon fibre elastic stiffness constants based on the composite and pure epoxy ultrasonic measurements.

	E_{11} (GPa)	ν_{12}	E_{22} (GPa)	ν_{23}	G_{12} (GPa)
	225	0.335	17.7	0.295	15.5

Table 4: The predicted AS4 carbon fibre engineering constants based on the composite and pure epoxy ultrasonic measurements.

It is encouraging that the derived value for the longitudinal Young's modulus of the carbon fibre (E_{11}) is in good agreement to that of the manufacturer's value shown in Table 1.

Having determined the carbon fibre elastic constants for the volume fraction of the experimental material, the composite elastic properties (at a frequency of 2.25MHz) can now be determined for any fibre volume fraction. These results are shown in Figure 7, where the symbols show the experimentally determined composite constants.

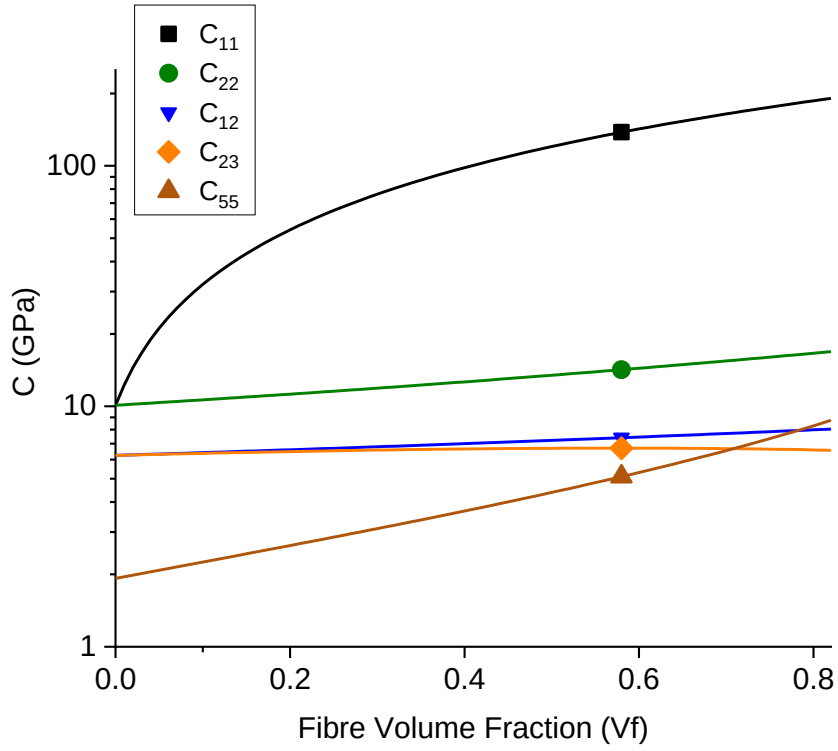

Figure 7: The predicted variation of the composite stiffness constants with fibre volume fraction. The experimental measurements (Vf = υ_2 = 0.58) are shown as symbols.

4.2 Measuring the viscoelastic constants of the unidirectional carbon fibre epoxy composite at 1Hz

4.2.1 Pure epoxy measurements at 1Hz

Having determined the elastic constants of the carbon fibres, the aim was then to predict the viscoelastic constants of the carbon fibre/epoxy composite. Here, the viscoelastic properties come only from the 913 epoxy matrix (the carbon fibres are assumed to be purely elastic) and so the first stage is to measure the pure epoxy viscoelastic properties. For obtaining the viscoelastic predictions, both the elastic component and the viscoelastic component are required for two independent elastic constants. Here we have carried out testing in three-point bend to measure E′ and tanδ, and testing in rectangular torsion to measure G′ and tanδ. Both test were carried out at a frequency of 1Hz and at a temperature of 20°C.

Table 5 shows the results of these measurements, including the uncertainties in the measurements from 5 repeated tests for each geometry. Again it is encouraging that the measured storage Young's modulus is close to that of the manufacturers value shown in Table 1.

	Storage modulus (GPa)	$\tan\delta$	Test Method
torsion	$G' = 1.32 \pm 0.03$	0.014 ± 0.001	Rectangular torsion measurements
bending	$E' = 3.56 \pm 0.09$	0.016 ± 0.001	Dual cantilever beam

Table 5: Measured viscoelastic properties of the pure 913 epoxy resin using DMA measurements at a frequency of 1Hz.

4.2.2: Unidirectional composite measurements

Steel calibration

As the composite is expected to have a much higher longitudinal Young's modulus and much lower $\tan\delta$ than the pure epoxy resin, it was necessary to first measure the intrinsic stiffness and any internal energy loss of the DMTA apparatus, using a steel calibration sample. This has a known Young's Modulus of 210GPa and is expected to be practically purely elastic ($\tan\delta = 0$).

To carry out a dynamic test in bending, the sample has to be subjected to a preload that is greater than the amplitude of that produced by the chosen dynamic strain. Table 6 shows results for the measured Young's modulus and tanδ of the steel sample at three different preloads of 300, 600 and 800g using a strain amplitude of 0.005%. The results in Table 6 show that as the preload is increased, the Young's modulus increases and the $\tan\delta$ decreases significantly. We attribute this to the increased preload forcing the sample to sit flatter on the knife-edges of the three-point bend fixtures and thus reducing contact friction. It is well known that if the sample does not sit perfectly flat on the testing fixture, then this can cause frictional losses that will

show up as an increased tanδ. As the maximum load range of the machine is 1000g, we have used a preload of 800g for all the subsequent measurements of the pure epoxy and the composite sample. Even with a high preload, the measured Young's modulus did still not reach the expected value of 210GPa. We attribute this to machine compliance, and have corrected all the subsequent measurements with this small machine internal displacement.

Preload (g)	Strain amplitude (%)	E′ (GPa)	tanδ
300	0.005	193	0.0035
600	0.005	198	0.0007
800	0.005	201	0.0001

Table 6: The effect of preload on the real part of Young's modulus and tanδ - three-point bend geometry.

4.2.3 Experimental measurements of the viscoelastic constants of the composite samples

Following the calibration, three-point bend measurements were carried out on composite samples cut along the two principal in-plane directions (Longitudinal (1) in the fibre direction and transverse (2) perpendicular to the fibres). Table 7 shows these experimental measurements for the Young's modulus and tanδ in these two directions. As expected, the Young's modulus is significantly higher in the fibre (1) direction, associated with a very low tanδ, with the opposite trend in the transverse (2) direction.

	E′ (GPa)	tanδ	comments
E_{11}	123 ± 1	0.0006 ± 0.0001	Measurement
	133.0 ± 0.04	0.00020 ± 0.00004	Prediction
E_{22}	8.28 ± 0.05	0.012 ± 0.001	Measurement
	8.4 ± 0.7	0.013 ± 0.02	Prediction

Table 7: A comparison of the measured and predicted viscoelastic composite properties using the three-point geometry.

4.2.4 Comparing micromechanical predictions with the experimental measurements

Micromechanical predictions for the same two engineering constants are also shown in Table 7 alongside the experimental measurements. The inputs for this calculation are the carbon fibre elastic constants (which are assumed to be frequency independent, Table 3) and the epoxy resin viscoelastic constants (Table 5). It is seen that in general, the agreement between the predictions and the experimental measurements is excellent. The uncertainties shown for the micromechanical predictions were formed by determining the effect of the extreme ranges of the uncertainties of the input epoxy resin properties (Table 5) on the final predictions. For the transverse properties (E_{22} and $\tan\delta$) the agreement between experimental measurements and predictions is within the uncertainty ranges of the various values. For the longitudinal properties (E_{11} and $\tan\delta$) the agreement is close, but not within the uncertainty ranges. It could be suggested that the experimental measurements for this longitudinal direction are at the extremes of such measurements (very high stiffness and very low loss) and so we could hypothesise that the micromechanical predictions are more reliable.

Following on from this comparison, the micromechanical model can now be used to determine both the viscoelastic stiffness constants (Table 8) and the five viscoelastic engineering constants (Table 9), for the unidirectional carbon fibre reinforced epoxy resin composite (Vf = 0.58).

	Real part (GPa)	Imaginary part (GPa)
C_{11}	135.4 ± 1.5	0.110 ± 0.063
C_{12}	5.02 ± 1.75	0.111 ± 0.069
C_{22}	10.35 ± 2.01	0.170 ± 0.080
C_{23}	4.42 ± 1.91	0.111 ± 0.075
C_{55}	3.847 ± 0.068	0.0420 ± 0.0035

Table 8: Predictions for all five stiffness constants (real and imaginary parts). Ranges based on the measurements uncertainty ranges for the epoxy resin sample (Table 5).

	Real part	Imaginary part
E_{11} [GPa]	132.95 ± 0.04	0.0240 ± 0.003
E_{22} [GPa]	8.4 ± 0.7	0.11 ± 0.02
G_{12} [GPa]	3.85 ± 0.07	0.0420 ± 0.004
G_{23} [GPa]	2.97 ± 0.06	0.030 ± 0.003
ν_{12}	0.34 ± 0.03	0.0010 ± 0.0002

Table 9: Predictions for all five independent viscoelastic engineering constants. Ranges based on the measurements uncertainty ranges for the epoxy resin sample (Table 5).

As only four of these ten independent components can be easily determined experimentally, this is a significant contribution, offering a full set of viscoelastic constants for designers to

utilise for optimising the vibration damping and noise cutting design of advanced engineering structural parts from unidirectional carbon fibre composite materials.

As a final comment, in this work, the classical micromechanical Hashin-Rosen composite cylinders model was used to calculate the fiber elastic moduli needed to produce the ultrasonically measured composite elastic moduli and the same model is then used to calculate the low frequency stiffness moduli. Other models, such as, for example, the self-consistent scheme [35-37] or the semi-empirical Halpin-Tsai equations [38], may also be used. As long as the same model is employed to calculate both fiber and composite moduli, the predicted composite moduli may be expected to be reasonably accurate. However, given that the composite cylinders model has been convincingly validated in our recent works on viscoelastic properties of unidirectional composites [11, 31], there seems to be no obvious reason for us for not adopting this validate classical micromechanical model in our present study.

5 Conclusions

In this paper a new micromechanical modelling scheme was presented for predicting all five independent viscoelastic constants of a unidirectional carbon fibre reinforced epoxy resin composite. Two crucial aspects in any modelling study are first to base the predictions on representative input values and secondly, and most importantly, to validate the final model predictions against experimental viscoelastic measurements.

For the first aspect, the five elastic constants of the reinforcing carbon fibres were determined by combining experimental ultrasonic immersion measurements of the composite and the pure epoxy matrix resin with a previously validated elastic micromechanical model. For the second aspect, namely the prediction and validation of the viscoelastic properties of the composite, these experimentally determined carbon fibre elastic constants were then used as model inputs together with the experimentally measured viscoelastic properties of the epoxy resin. The micromechanical modelling scheme utilised classical Hashin-Rosen composite cylinders model and used the elastic-viscoelastic correspondence principle to convert the static elastic solutions to their complex steady state viscoelastic forms simply by replacing static elastic moduli of the matrix and the fibres by the complex viscoelastic moduli measured at two different oscillation frequencies.

Validation of the proposed micromechanical modelling scheme was achieved by experimentally measuring the elastic and viscoelastic components for two of the five independent engineering constants. These were the longitudinal Young's modulus and its $\tan\delta$ plus the transverse Young's modulus and its $\tan\delta$. Excellent agreement was found between the micromechanical predictions and the experimental measurements for these four constants. The powerful aspects of the validated model is that it can then be used to predict the elastic and viscoelastic components for all five engineering constants, all of which are required for

accurate design of the vibrational damping and noise cutting performance of advanced engineering structures from these composite materials.

References

[1] F. Andersson, A. Hagqvist, E. Sundin, M. Bjorkman, Design for Manufacturing of Composite Structures for Commercial Aircraft - the Development of a DFM strategy at SAAB Aerostructures, in: H. ElMaraghy (Ed.), Variety Management in Manufacturing: Proceedings of the 47th Cirp Conference on Manufacturing Systems2014, pp. 362-367.

[2] M.R. Future,Global Automotive Carbon Fiber Composites Market Research Report - Forecast to 2023, 2018

[3] X.D. Yang, L.Y. Sun, C. Zhang, L.J. Li, Z.M. Dai, Z.K. Xiong, Design and Optimization of Composite Automotive Hatchback Using Integrated Material-Structure-Process-Performance Method, Applied Composite Materials 25(6) (2018) 1455-1475.

[4] A. Sohouli, M. Yildiz, A. Suleman, Cost analysis of variable stiffness composite structures with application to a wind turbine blade, Composite Structures 203 (2018) 681-695.

[5] O. Karacali, Mechanical Analysis of a 1.2 MW-40 m Long Horizontal Axis Composite Material Wind Turbine Blade by S-N Fatigue Cycle and Goodman Diagrams in Windpower Engineering, Acta Physica Polonica A 134(1) (2018) 394-396.

[6] J. Simpson, J. Schweiger, An industrial approach to piezo electric damping of large fighter aircraft components, in: J.M. Sater (Ed.), Industrial and Commercial Applications of Smart Structures Technologies - Smart Structures and Materials 1998, Spie-Int Soc Optical Engineering, Bellingham, 1998, pp. 34-46.

[7] S.W. Tsai, H.T. Hahn, Introduction to Composite Materials, Technomic Publishing Company Inc., Lancaster, Pennsylvania, 1980.

[8] J.N. Reddy, Mechanics of Laminated Composite Plates and Shells (second edition), CRC Press, Taylor and Francis Group, Boca Raton, FL, 2004.

[9] J.N. Reddy, Theory and Analysis of Elastic Plates and Shells (second edition), CRC Press, Taylor and Francis Group, Boca Raton, FL., 2006.

[10] R.M. Christensen, Theory of Viscoelasticity, 2nd ed., Academic Press, New York, 1982.

[11] A.A. Gusev, L.S. Kern, Frequency domain finite element estimates of viscoelastic stiffness of unidirectional composites, Composite Structures 194 (2018) 445-453.

[12] A.A. Gusev, Time domain finite element estimates of dynamic stiffness of viscoelastic composites with rigid spherical inclusions, International Journal of Solids and Structures 88-89 (2016) 79-97.

[13] A.A. Gusev, Controlled accuracy finite element estimates for the effective stiffness of composites with spherical inclusions, International Journal of Solids and Structures 80 (2016) 227-236.

[14] A.A. Gusev, Optimum microstructural design of coated sphere filled viscoelastic composites for structural noise and vibration damping applications, International Journal of Solids and Structures 128 (2017) 1-10.

[15] R.E. Smith, Ultrasonic elastic constants of carbon fibers and their composites, Journal of Applied Physics 43 (1972) 2555-2611.

[16] HexTow® AS4 Carbon Fiber. https://www.hexcel.com/user_area/content_media/raw/AS4_HexTow_DataSheet.pdf. (Accessed 22/01/2019 2019).

[17] HexPly® 913, 125°C curing epoxy matrix. https://www.hexcel.com/user_area/content_media/raw/HexPly_913_eu_DataSheet.pdf. (Accessed 22/01/2019 2019).

[18] B.E. Read, G.D. Dean, The determination of the dynamic properties of polymers and composites, Adam Hilger, Bristol, 1978.

[19] S.R.A. Dyer, D. Lord, I.J. Hutchinson, I.M. Ward, R.A. Duckett, J.Phys.D.Appl.Phys 25(66) (1992).

[20] D. Lord, The determination of the elastic constants of fibre reinforced composites by an ultrasonic method, University of Leeds, Leeds, 1980.

[21] M.F. Markham, Measurement of the elastic constants of fibre composites by ultrasonics, Composites 1 (1970) 145-149.

[22] J.F. Clarke, R.A. Duckett, P.J. Hine, I.J. Hutchinson, I.M. Ward, Negative Poissons Ratios in Angle-Ply Laminates - Theory and Experiment, Composites 25(9) (1994) 863-868.
[23] M. Landert, A. Kelly, R.J. Stearn, P.J. Hine, Negative thermal expansion of laminates, Journal of Materials Science 39(11) (2004) 3563-3567.
[24] P.J. Hine, I.M. Ward, Measuring the elastic properties of high-modulus fibres, Journal of Materials Science 31(2) (1996) 371-379.
[25] B. Brew, P.J. Hine, I.M. Ward, The properties of PIPD-fibre/epoxy composites, Composites Science and Technology 59(7) (1999) 1109-1116.
[26] A.A. Gusev, P.J. Hine, I.M. Ward, Fiber packing and elastic properties of a transversely random unidirectional glass/epoxy composite, Composites Science and Technology 60(4) (2000) 535-541.
[27] Z. Hashin, B.W. Rosen, The elastic moduli of fiber-reinforced materials, Journal of Applied Mechanics 31 (1964) 223-232.
[28] Z. Hashin,Theory of fiber reinforced materials, NASA CR-1974, 1972
[29] Z. Hashin, Analysis of composite materials - A survey, Journal of Applied Mechanics 50 (1983) 481-505.
[30] R.M. Christensen, K.H. Lo, Solutions for effective shear properties in 3 phase sphere and cyclinder models, Journal of the Mechanics and Physics of Solids 27(4) (1979) 315-330.
[31] L.S. Kern, P.J. Hine, A.A. Gusev, Optimizing the damping properties of unidirectional composites by incorporating carbon fibers with a thin viscoelastic coating, Composite Structures 208 (2019) 879-890.
[32] A.P. Unwin, P.J. Hine, I.M. Ward, M. Fujita, E. Tanaka, A.A. Gusev, Novel phase separated multi-phase materials combining high viscoelastic loss and high stiffness, Composites Science and Technology 167 (2018) 106-114.
[33] A.P. Unwin, P.J. Hine, I.M. Ward, M. Fujita, E. Tanaka, A.A. Gusev, Escaping the Ashby limit for mechanical damping/stiffness trade-off using a constrained high internal friction interfacial layer, Scientific Reports 8(1) (2018) 2454.
[34] A.A. Gusev, Effective coefficient of thermal expansion of n-layered composite sphere model: Exact solution and its finite element validation, International Journal of Engineering Science 84 (2014) 54-61.
[35] R. Hill, THEORY OF MECHANICAL PROPERTIES OF FIBRE-STRENGTHENED MATERIALS .3. SELF-CONSISTENT MODEL, Journal of the Mechanics and Physics of Solids 13(4) (1965) 189-+.
[36] J.J. Hermans, The Elastic Properties of Fiber Reinforced Materials When the Fibers are Aligned, Proceedings Koninklijke Nederlandse Akademie van Wetenschappen, Series B, 1967, pp. 1-9.
[37] Kerner E.H., The Elastic and Thermoelastic Properties of Composite Media, Proceedings of the Physical Society, Vol B 69, 1956, pp. 807-808.
[38] J.E. Ashton, J.C. Halpin, Petit. P.H., Primer on Composite mateirlas, Chapter 5, Technomic1969.